Time dependences of two-, three-, and four-photon ionization of atomic hydrogen in the ground 1^2S and metastable 2^2S states

Craig R. Holt*

Department of Physics, University of Colorado, Boulder, Colorado 80309

M. G. Raymer† and William P. Reinhardt

Department of Chemistry, University of Colorado, Boulder, Colorado 80309
and Joint Institute for Laboratory Astrophysics, University of Colorado and
National Bureau of Standards, Boulder, Colorado 80309

The two-level model of multiphoton ionization is reviewed within the context of an exact theoretical framework. Parametrization of the complex dressed states arising in a generalized Floquet analysis gives numerical values for the effective two-level parameters for two-, three-, and four-photon ionization of ground-state atomic hydrogen with the $(m_l=0)$ intermediate resonant states $2p$, $2s$, and $3p$, respectively. Detailed time dependences of the ionization process are given for responses to a linearly polarized, monochromatic, single-mode laser turned on suddenly with respect to near-resonant states, but adiabatically with respect to all others. Appropriate expressions for time-independent ionization rates are obtained during specific time intervals. The K index $(K = \partial \ln N / \partial \ln I)$, of interest in recent experiments, is understood within the framework of a simple model. Application to four-photon ionization of the metastable $^2S_{1/2}$ state of hydrogen illustrates the breakdown of the two-level model, as the number of "near-resonant" levels is a function of the field strength.

I. INTRODUCTION

In certain circumstances two- (or more-) photon ionization of a system with one intermediate resonant state may be modeled as a two-level system, via a time-independent 2×2 non-Hermitian Hamiltonian. The imaginary parts of the diagonal elements simulate loss of population from the bound states into one or more continua. If the matrix elements of the 2×2 Hamiltonians are known as a function of intensity and frequency, then ionization rates and cross sections are obtained by solving the time-dependent Schrödinger equation.

Alternatively, all the levels (bound *and* continuum) can be taken into account in a generalized Floquet formulation of the multiphoton process.[1] The dilatation transformation $r \rightarrow re^{i\theta}$ is applied to the Floquet Hamiltonian in order to obtain complex eigenvalues corresponding to complex dressed states. These eigenvalues and their eigenvectors are used to obtain ionization probabilities from which ionization rates are extracted.

In this paper we make the connection between these two approaches. Algebraic expressions are obtained which identify eigenvalues and eigenvectors of the generalized Floquet model with the parameters appearing in a two-level model. Converged numerical values for the eigenvalues and eigenvectors of the Floquet Hamiltonian obtained for atomic systems can thus be used to generate the two-level parameters. Neglect of all but the two dominant Floquet eigenvalues (eigenstates) assumes that only two bound levels are in resonance and is equivalent to an adiabatic square-pulse turn-on of the laser,[2] as is discussed in Sec. VII.

We have carried out this program for atomic hydrogen in which two-, three-, and four-photon ionization of the 1^2S, or "$1s$," state is considered in the nonrelativistic limit. Having calculated the appropriate parameters, we employ the two-level model to obtain ionization probabilities as a function of time and, under special conditions, time-independent ionization rates. In addition, we have studied the K-index plots for the above systems, where $K = \partial \ln N / \partial \ln I$, N being the number of ionization events per laser pulse of intensity I.[3] K is of interest as it shows considerable structure as a function of laser detuning from resonance and thus is an experimentally accessible frequency-domain probe of the detailed time dependence of the ionization event. In all of the above cases, the two-level model is entirely adequate to represent the results of the generalized Floquet theory.

A two-level model will certainly break down if

more than one level is in resonance simultaneously. However, the notation of which states are near enough to resonance may depend on the laser intensity. An interesting example occurs in the four-photon ionization of the metastable 2^2S, or "$2s$," state of atomic hydrogen where at low intensities a two-level model is adequate to model the system, while at higher intensity a formerly off-resonant level is power broadened into resonance necessitating use of a more sophisticated model.

The plan of the paper is as follows: In Sec. II we review the two-level model and derive its connection (Sec. III) with the generalized Floquet theory, with specific application to atomic hydrogen. Avoided crossings of the two-level eigenvalues are discussed in Sec. IV for the three cases $\Omega \gg \gamma/2$, $\Omega \approx \gamma/2$, and $\Omega \ll \gamma/2$, Ω being an effective Rabi frequency and γ the upper-state ionization rate. It is seen that the two-, three-, and four-photon ionization processes considered give representative examples of these three cases. The implications for the time dependences of the ionization process and for the K-index detuning plots of these three basic cases are discussed in Secs. V and VI. Section VII contains the results of analysis of the four-photon ionization of the hydrogenic $2s$ state and the breakdown of the two-level model explored. Finally, Sec. VIII contains a brief summary and discussion.

II. TWO-LEVEL MODEL

The two-level model[4] of N-photon ionization entails use of a time-independent 2×2 Hamiltonian H, whose matrix elements have a specific form and physical interpretation. H is defined by

$$H = \begin{bmatrix} h_{11} & h_{12} \\ h_{21} & h_{22} \end{bmatrix} ,$$ (1)

where (in a.u.)

$$h_{11} = E_1^{(0)} + \delta_1 - i\frac{\gamma_1}{2} ,$$ (2a)

$$h_{22} = E_1^{(0)} + \delta_2 - (N-1)\omega - i\frac{\gamma_2}{2} ,$$ (2b)

$$h_{12} = h_{21} = -\frac{\Omega + i\beta}{2} .$$ (2c)

The laser is assumed to be monochromatic and linearly polarized with electric field amplitude $\vec{\epsilon} = \vec{E}\cos(\omega t)$. $E_1^{(0)}$ ($E_2^{(0)}$) is the unperturbed atomic energy, δ_1 (δ_2) is the ac Stark shift due to levels other than $|2\rangle$ ($|1\rangle$), and γ_1 (γ_2) is the ionization width of $|1\rangle$ ($|2\rangle$). To lowest order in perturbation theory the field dependences of these parameters are as follows: δ_1 and δ_2 are proportional to E^2 as ex-

pected from the second-order theory of ac Stark shifts; γ_1 is proportional to E^{2N} because it describes a direct N-photon ionization of $|1\rangle$ via levels other than $|2\rangle$; γ_2 is proportional to E^2 because it describes a one-photon ionization of $|2\rangle$. Ω, the effective Rabi frequency, describes, in lowest order, a process whereby the atom undergoes a transition from $|1\rangle$ to $|2\rangle$ by absorption of $N-1$ photons; thus Ω is proportional to E^{N-1}. β describes a virtual process whereby the atom undergoes a transition from $|1\rangle$ to $|2\rangle$ via the continuum. N photons take the atom to a continuum state, followed by emission of a photon leaving the atom in $|2\rangle$; thus β is proportional to E^{N+1} (see Fig. 1 and Table I).

The time evolution of an initial state (assuming dephasing mechanisms, such as collisions, spontaneous emission, etc., are negligible) follows from the solution of the Schrödinger equation

$$H\psi(t) = i\frac{\partial}{\partial t}\psi(t) ,$$ (3)

where

$$\psi(t) = \begin{bmatrix} a_1(t) \\ a_2(t) \end{bmatrix} ,$$ (4)

TWO-PHOTON IONIZATION PARAMETERS

N-PHOTON IONIZATION PARAMETERS
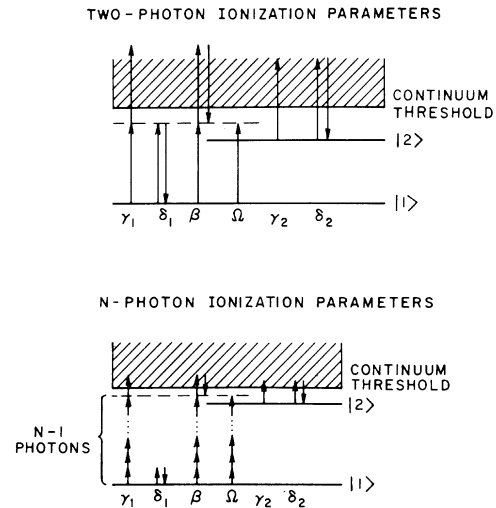
FIG. 1. Virtual processes contributing to perturbative calculations of the two- and N-photon ionization parameters. Above contributions to γ_1 and δ_1 would be calculated perturbatively using all levels except $|2\rangle$. This is indicated schematically by the absence of the solid line representing $|2\rangle$. For β, the calculation of the N-photon transition to the continuum states neglects $|2\rangle$, but the one-photon transition from the continuum to $|2\rangle$ retains state $|2\rangle$ in the calculation. Similarly, the calculation of this contribution to γ_2 and δ_2 would neglect level $|1\rangle$. Calculation of Ω would neglect neither $|1\rangle$ nor $|2\rangle$. This figure, along with Table I, allows the power dependences of the two-level parameters to be determined (to lowest order in perturbation theory).

TABLE I. Lowest-order perturbative expressions for the two-level parameters describing a two-photon ionization process, where only one continuum state $|\alpha\rangle$ is assumed (Ref. 7). Field dependences are extracted and, with the help of Fig. 1, generalized for the N-photon case. Subscripts beneath the integral symbols indicate which states are neglected in the Stiltjes integral.

Two-photon ionization parameters	N-photon Ionization parameters
$\Omega = \langle 1 \| \vec{r}\cdot\vec{E} \| 2 \rangle \propto E$	$\Omega \propto E^{N-1}$
$\gamma_2 = 2\pi \| \langle 2 \| \vec{r}\cdot\vec{E} \| \alpha \rangle \|^2 \propto E^2$	$\gamma_2 \propto E^2$
$\delta_1 = P \displaystyle\int_2 \frac{\|\langle 1 \| \vec{r}\cdot\vec{E} \| \mu \rangle\|^2 d\sigma(\mu)}{E_1 - E_\mu + 2\omega} \propto E^2$	$\delta_1 \propto E^2$
$\delta_2 = P \displaystyle\int_1 \frac{\|\langle 2 \| \vec{r}\cdot\vec{E} \| \mu \rangle\|^2 d\sigma(\mu)}{E_2 - E_\mu + 2\omega} \propto E^2$	$\delta_2 \propto E^2$
$\gamma_1 = 2\pi \left\| \displaystyle\int_2 \frac{\langle 1 \| \vec{r}\cdot\vec{E} \| \mu \rangle \langle \mu \| \vec{r}\cdot\vec{E} \| \alpha \rangle}{E_1 - E_\mu - \omega} d\sigma(\mu) \right\|^2 \propto E^4$	$\gamma_1 \propto E^{2N}$
$\beta = (\gamma_1 \gamma_2)^{1/2} \propto E^3$	$\beta \propto E^{N+1}$

or

$$\underline{\psi}(t) = a_1(t) | 1, n \rangle + a_2(t) | 2, n - N + 1 \rangle , \quad (5)$$

where n refers to the number of photons in the field. The initial conditions $a_1(0) = 1$ and $a_2(0) = 0$ generate the solutions

$$a_1(t) = \frac{\lambda_A - h_{22}}{\lambda_A - \lambda_B} e^{-i\lambda_A t} - \frac{\lambda_B - h_{22}}{\lambda_A - \lambda_B} e^{-i\lambda_B t} , \quad (6a)$$

$$a_2(t) = \frac{h_{12}}{\lambda_A - \lambda_B} (e^{-i\lambda_A t} - e^{-i\lambda_B t}) , \quad (6b)$$

where the eigenvalues λ_A and λ_B of H are given by

$$\lambda_A = \frac{h_{11} + h_{22}}{2} + \frac{1}{2} [(h_{22} - h_{11})^2 + 4h_{12}^2]^{1/2} , \quad (7a)$$

$$\lambda_B = \frac{h_{11} + h_{22}}{2} - \frac{1}{2} [(h_{22} - h_{11})^2 + 4h_{12}^2]^{1/2} . \quad (7b)$$

The number of ions is proportional to the probability $C(t)$ of finding an electron in a continuum state; $C(t)$ is given in the two-level model by

$$C(t) = 1 - |a_1(t)|^2 - |a_2(t)|^2 . \quad (8)$$

A study of $C(t)$ as a function of time and laser frequency provides information on the ionization process.

Before the model can be applied to real atomic systems, numerical values of the two-level parameters are needed. These are obtained by fitting to the coupled dressed Floquet eigenvalues of Sec. III.

III. GENERALIZED FLOQUET THEORY AND ITS CONNECTION WITH THE STANDARD TWO-LEVEL MODEL

Floquet theory is an alternative method for treating multiphoton processes. In principle, it allows one to solve exactly for the time evolution of a many-level quantum system under the influence of a periodic external perturbation, without using perturbation theory or the rotating-wave approximation. In this section it will be shown that, under certain conditions, the generalized many-level—plus—continuum Floquet theory of Maquet, Chu, and Reinhardt[1] (MCR) reduces to a two-level description. The connection with the standard two-level model is made and explicit relations between the two-level parameters and Floquet eigenvalues are given. Finally, we show how to generate the Floquet eigenvalues numerically, in the special case of atomic hydrogen.

A. Review of Floquet theory

A detailed exposition of Floquet theory for systems with discrete energy levels can be found in the paper by Shirley.[1] Extensions allowing inclusion of continuous spectra have been made by Chu and Reinhardt[1] and in MCR.[1] We will review only those parts of the theory necessary to analyze an N-photon ionization process.

We first describe the form of the laser pulse assumed in the ionization process. We take the pulse to be essentially a square pulse, but with (brief) rise and fall times which make it adiabatic with respect to the nonresonant atomic states, while remaining sudden with respect to the near-resonant state $|2\rangle$. This means that the rise and fall times must be long

compared to the inverse of the laser detuning with all far-off-resonance states, but short compared to the response times Δ^{-1}, Ω^{-1}, and γ_2^{-1} of the near-resonant states $|2\rangle$. For the near-resonant problem under consideration, this type of pulse[2] has temporal properties similar to those of experimentally obtainable pulses.

Floquet theory, along with the above adiabatic square-pulse assumption,[2] provides an expression for the ionization probability. Given that the atom is in state $|\alpha\rangle$ at $t=0$, we denote the probability of finding the atom in the state $|\beta\rangle$ by $P_{\alpha\to\beta}(t)$. Then the probability of finding the system in a continuum state is given by[1]

$$C(t)=1-\sum_{\beta}P_{\alpha\to\beta} , \tag{9}$$

where the sum over β includes all bound states. Far-off-resonant levels are not appreciably populated due to the adiabatic nature of the pulse; thus the sum over β in Eq. (9) can be truncated to two terms,

$$C(t)\cong 1-P_{1\to1}-P_{1\to2} , \tag{10}$$

where $|1\rangle$ denotes the initial state $|\alpha\rangle$, and $|2\rangle$ denotes the intermediate state, as in Fig. 1.

The probabilities $P_{1\to1}$ and $P_{1\to2}$ can be evaluated from the Floquet theory, assuming a sudden turn-

on, as [see Eqs. (2.13) and (6.4) of MCR]

$$P_{1\to\beta}(t)=\sum_{m}|\langle\beta,m\,|e^{-iH_{\omega}^{\mathscr{F}}t}|\,1,n\rangle|^{2} ,$$

$$\beta=1,2 . \tag{11}$$

Here $|\beta,m\rangle$ is a direct product state with β referring to the unperturbed atomic state and m referring to the number of photons in the field; $H_{\omega}^{\mathscr{F}}$ is the Floquet Hamiltonian, which we treat in the dipole approximation. The sum over m indicates that we are not interested in the final state of the photon field. The states $|\beta,m\rangle$ (the bare states) are to be distinguished from the eigenstates $|\epsilon\rangle$ (the dressed states) of the Floquet Hamiltonian, defined by

$$H_{\omega}^{\mathscr{F}}|\epsilon\rangle=\epsilon|\epsilon\rangle . \tag{12}$$

The ionization probability $C(t)$ may now be written as

$$C(t)=1-\sum_{m}|\langle1,m\,|e^{-iH_{\omega}^{\mathscr{F}}t}|\,1,n\rangle|^{2}$$
$$-\sum_{m}|\langle2,m\,|e^{-iH_{\omega}^{\mathscr{F}}t}|\,1,n\rangle|^{2} . \tag{13}$$

Given the eigenstates $|I\rangle$ and eigenvalues ϵ_I of $H_{\omega}^{\mathscr{F}}$, a resolution of the identity may be inserted into Eq. (13), yielding

$$C(t)=1-\sum_{m}\int d\epsilon\,|\langle1,m\,|\epsilon\rangle\langle\epsilon|\,1,n\rangle e^{-i\epsilon t}|^{2}-\sum_{m}\int d\epsilon\,|\langle2,m\,|\epsilon\rangle\langle\epsilon|\,1,n\rangle e^{-i\epsilon t}|^{2} , \tag{14}$$

where the integration $\int d\epsilon$ run over the (continuous) spectrum of $H_{\omega}^{\mathscr{F}}$.

B. Reduction to two levels

In this section, additional assumptions are made and used to approximate Eq. (14). Only two direct product states are expected to be populated: $|1,n\rangle$ and $|2,n-N+1\rangle$. Population in $|2,n-N+3\rangle$, for example, results from an energy nonconserving process which we expect to be negligible. Accordingly, truncation of the sum over m in Eq. (14) results in

$$C(t)\cong 1-\int d\epsilon\,|\langle1,n\,|\epsilon\rangle\langle\epsilon|\,1,n\rangle e^{-i\epsilon t}|^{2}-\int d\epsilon\,|\langle2,n-N+1\,|\epsilon\rangle\langle\epsilon|\,1,n\rangle e^{i\epsilon t}|^{2} . \tag{15}$$

Similarly, only two states, labeled $|A\rangle$ and $|B\rangle$, are expected to be significantly populated. We thus expect Eq. (15) to be well approximated by

$$C(t)\cong 1-|\langle1,n\,|A\rangle\langle A\,|\,1,n\rangle e^{-i\lambda_A t}+\langle1,n\,|B\rangle\langle B\,|\,1,n\rangle e^{-i\lambda_B t}|^{2}$$
$$-|\langle2,n-N+1\,|A\rangle\langle A\,|\,1,n\rangle e^{-i\lambda_A t}+\langle2,n-N+1\,|B\rangle\langle B\,|\,1,n\rangle e^{-i\lambda_B t}|^{2} . \tag{16}$$

As discussed in detail in MCR, derivation of Eq. (16) requires a contour distortion of the integration path in Eqs. (14) and (15), resulting in the fact that λ_A (λ_B) and $|A\rangle$ ($|B\rangle$) are the complex eigenvalues and eigenvectors of the analytically continued (non-Hermitian) Floquet Hamiltonian $H_{\omega}^{\mathscr{F}}(\theta)$,

$$H_{\omega}^{\mathscr{F}}(\theta)|I\rangle=\lambda_I|I\rangle, \quad I=A,B . \tag{17}$$

The states $|A\rangle$ and $|B\rangle$ are the (complex) dressed states which provide correspondence with the two-level Hamiltonian of Eqs. (3) and (4).

These truncations lead naturally to a two-level ap-

proximation of the full atomic system. This approximation is to be contrasted to the usual rotating-wave approach in which the Hamiltonian is first approximated and $C(t)$ is obtained by solving the resulting Schrödinger equation. Our approach is to start from the rigorous Floquet solutions and neglect certain terms which are expected to be small on intuitive grounds. The numerical calculations of Sec. IV fully justify this procedure.

C. Parameter identification

The parameters appearing in the two-level model can be identified with the Floquet theory by comparing the forms of $C(t)$ in Eqs. (6) and (16). In the preceding discussion $P_{1\rightarrow 2}(t)$ corresponds to $|a_2(t)|^2$ and $P_{1\rightarrow 1}(t)$ corresponds to $|a_1(t)|^2$; thus we equate

$$a_1(t) = \langle 1,n \mid A \rangle \langle A \mid 1,n \rangle e^{-i\lambda_A t}$$
$$+ \langle 1,n \mid B \rangle \langle B \mid 1,n \rangle e^{-i\lambda_B t} , \qquad (18a)$$

$$a_2(t) = \langle 2,n-N+1 \mid A \rangle \langle A \mid 1,n \rangle e^{-i\lambda_A t}$$
$$+ \langle 2,n-N+1 \mid B \rangle \langle B \mid 1,n \rangle e^{-i\lambda_B t} , \qquad (18b)$$

where λ_A has been identified with μ_A and λ_B with μ_B. By identifying $a_1(t)$ and $a_2(t)$ appearing in (18a) and (18b) with $a_1(t)$ and $a_2(t)$ appearing in (7a) and (7b) we obtain the following relations:

$$\langle A \mid 1,n \rangle^2 = \frac{\mu_A - h_{22}}{\mu_A - \mu_B} , \qquad (19a)$$

$$\frac{\langle A \mid 2,n-N+1 \rangle}{\langle A \mid 1,n \rangle} = \frac{h_{12}}{\mu_A - h_{22}} , \qquad (19b)$$

$$\langle B \mid 1,n \rangle^2 = -\frac{\mu_B - h_{22}}{\mu_A - \mu_B} , \qquad (19c)$$

$$\frac{\langle B \mid 2,n-N+1 \rangle}{\langle B \mid 1,n \rangle} = \frac{h_{12}}{\mu_B - h_{22}} . \qquad (19d)$$

Solving for the h_{ij}'s, using $\mu_A = \lambda_A$ and $\mu_B = \lambda_B$, we see that

$$h_{12} = (\lambda_A - \lambda_B)\langle A \mid 1,n \rangle \langle A \mid 2,n-N+1 \rangle , \qquad (20a)$$

$$h_{11} = \frac{\lambda_A + \lambda_B}{2} - \frac{1}{2}[(\lambda_A - \lambda_B)^2 - 4h_{12}^2]^{1/2} , \qquad (20b)$$

$$h_{22} = \frac{\lambda_A + \lambda_B}{2} + \frac{1}{2}[(\lambda_A - \lambda_B)^2 - 4h_{12}^2]^{1/2} , \qquad (20c)$$

where use has been made of the fact that $\langle a,n \mid A \rangle = \langle A \mid a,n \rangle$. This is a result of $H_\omega^{\mathcal{F}}(\theta)$ being complex symmetric and thus having left and right eigenvectors which are simply the transpose of one another rather than the more usual Hermitian conjugates (see the Appendix). Once the coefficients $\langle A \mid 1,n \rangle$, $\langle A \mid 2,n-N+1 \rangle$, $\langle B \mid 1,n \rangle$, $\langle B \mid 2,n-N+1 \rangle$, and the eigenvalues λ_A and λ_B are known, they can be used in Eqs. (20a)—(20c) to generate the parameters h_{ij} appearing in the two-level model.

D. Computational procedure

The non-Hermitian operator $H_\omega^{\mathcal{F}}(\theta)$ is obtained from $H_\omega^{\mathcal{F}}$ by the complex dilatation transformation $r \rightarrow re^{i\theta}$. $H_\omega^{\mathcal{F}}(\theta)$ has isolated eigenvalues in the lower half complex plane which correspond to the decaying dressed states. This is discussed more fully in MCR. $H_\omega^{\mathcal{F}}(\theta)$ is discretized using Laguerre functions,

$$r^{l+1}e^{-\lambda r/2}L_n^{2l+2}(\lambda r), \quad n=0,1,2,\dots \qquad (21)$$

appropriate to atomic bare states of angular symmetry l. Convergence of the matrix eigenvalues of $H_\omega^{\mathcal{F}}(\theta)$ with respect to the number of basis functions and number of Floquet blocks is as discussed in MCR. For the results discussed below typical calculations involve 400×400 complex symmetric matrices. As only a few of the $|I\rangle$ and λ_I are needed, inverse iteration is used to determine the complex λ_I nearest to estimated values, and full advantage is taken of the block symmetry of $\bar{H}_\omega^{\mathcal{F}}(\theta)$ as discussed in the appendix of MCR.

Matrix Floquet calculations have been carried out giving converged parameters for the two-, three-, and four-photon ionizaton of ground-state hydrogen with the $2p$, $2s$, and $3p$ $(m_l=0)$, respectively, as the near-resonant intermediate states. The complex Floquet amplitudes and eigenvalues yield the generalized two-level parameters shown in Table II.[5] The power dependence of these parameters, as revealed by the tables, is in good agreement with that predicted by the perturbative canonical two-level models. Note that for $E \lesssim 0.01$ a.u., $\Omega \gg \gamma_2$ for two-photon, $\Omega \sim \gamma_2$ for three-photon, and $\Omega \ll \gamma_2$ for four-photon ionization. In all three cases we have $\Omega, \gamma_2 \gg \beta, \gamma_1$. These inequalities follow from the power dependence of these parameters and are expected to hold for similar multiphoton processes. Limitations of numerical dynamic range made it impossible (except far off resonance) to obtain reliable values of γ_1 (which is very small) in the three- and four-photon cases. Even in the two-photon case, we find the anomalous increase of γ_1 near resonance to be due to numerical inaccuracies. Similarly, the

TABLE II. Two-level parameter in atomic units for (a) two-, (b) three-, and (c) four-photon ionization of ground-state hydrogen for several detunings and field strengths. ω, laser frequency; Δ, detuning; Ω Rabi frequency; β, imaginary Rabi frequency; γ_1 and γ_2 ionizaton widths of $|1\rangle$ and $|2\rangle$; δ_1 and δ_2, ac Stark shifts of $|1\rangle$ and $|2\rangle$; E, electric field amplitude. To a good approximation note that $\gamma_2, \delta_1, \delta_2 \propto E^2$; $\Omega \propto E^{N-1}$; $\beta \propto E^{N+1}$; $\gamma_1 \propto E^{2N}$, where N is the number of photons necessary for ionization. This is expected from lowest-order perturbation theory. Numerical accuracy prevented obtaining values for β and γ_1 in some instances. Only two reliable values of γ_1 were obtained in the three-photon case: $\gamma_1 = 5.7 \times 10^{-8}$ ($\omega = 0.185$ and $E = 0.01$) and $\gamma_1 = 5.0 \times 10^{-8}$ ($\omega = 0.195$ and $E = 0.01$). Peak field strength of $E = 1.0$ a.u. corresponds to an rms intensity of 3.51×10^{16} W/cm^2 for linearly polarized light; a circular frequency of 1.0 a.u. corresponds to 4.1341×10^{16} rad/sec.

ω	Δ	Ω	β	γ_1	γ_2	δ_1	δ_2
			(a)				
			$E = 0.001$ a.u.				
0.350	−2.500(−2)[a]	7.450(−4)	3.1(−9)	7.4(−11)	3.53(−7)	−9.33(−7)	3.36(−6)
0.360	−1.500(−2)	7.449(−4)	2.7(−9)	7.6(−11)	3.12(−7)	−9.79(−7)	3.18(−6)
0.370	−5.004(−3)	7.449(−4)	2.5(−9)	1.3(−10)	2.77(−7)	−1.04(−6)	3.01(−6)
0.375	−3.982(−6)	7.449(−4)	2.9(−9)	6.0(−10)	2.61(−7)	−1.07(−6)	2.92(−6)
0.380	4.996(−3)	7.449(−4)	3.2(−9)	1.0(−10)	2.46(−7)	−1.11(−6)	2.84(−6)
0.390	1.500(−2)	7.449(−4)	2.8(−9)	4.5(−11)	2.20(−7)	−1.21(−6)	2.70(−6)
0.400	2.500(−2)	7.449(−4)	2.4(−9)	3.3(−11)	1.97(−7)	−1.25(−6)	2.57(−6)
			$E = 0.005$ a.u.				
0.350	−2.511(−2)	3.727(−3)	3.9(−7)	4.6(−8)	8.80(−6)	−2.91(−5)	8.38(−5)
0.360	−1.510(−2)	3.726(−3)	3.5(−7)	4.8(−8)	7.77(−6)	−2.42(−5)	7.91(−5)
0.370	−5.099(−3)	3.725(−3)	3.2(−7)	6.8(−8)	6.87(−6)	−2.51(−5)	7.43(−5)
0.375	−9.711(−5)	3.723(−3)	3.6(−7)	9.1(−8)	6.45(−6)	−2.54(−5)	7.17(−5)
0.380	4.903(−3)	3.721(−3)	3.9(−7)	5.7(−8)	6.12(−6)	−2.70(−5)	7.03(−5)
0.390	1.490(−2)	3.720(−3)	3.4(−7)	2.9(−8)	5.48(−6)	−2.99(−5)	6.72(−5)
0.400	2.490(−2)	3.720(−3)	3.0(−7)	2.2(−8)	4.91(−6)	−3.34(−5)	6.40(−5)
			$E = 0.01$ a.u.				
0.350	−2.542(−2)	7.459(−3)	3.1(−6)	7.2(−7)	3.49(−5)	−8.95(−5)	3.32(−4)
0.360	−1.540(−2)	7.457(−3)	2.8(−6)	7.2(−7)	3.07(−5)	−9.25(−5)	3.12(−4)
0.370	−5.385(−3)	7.448(−3)	2.7(−6)	8.4(−7)	2.71(−5)	−9.43(−5)	2.91(−4)
0.375	−3.767(−4)	7.436(−3)	2.8(−6)	8.8(−7)	2.55(−5)	−9.59(−5)	2.81(−4)
0.380	4.624(−3)	7.423(−3)	2.9(−6)	7.3(−7)	2.41(−5)	−1.02(−4)	2.75(−4)
0.390	1.462(−2)	7.415(−3)	2.7(−6)	4.7(−7)	2.17(−5)	−1.16(−4)	2.65(−4)
0.400	2.462(−2)	7.412(−3)	2.4(−6)	3.5(−7)	1.95(−5)	−1.31(−4)	2.53(−4)
			(b)				
			$E = 0.001$ a.u.				
0.18500	−5.009(−3)	3.98(−6)			6.70(−6)	−1.42(−6)	7.65(−6)
0.18650	−2.009(−3)	3.95(−6)			6.52(−6)	−1.43(−6)	7.54(−6)
0.18700	−1.009(−3)	3.95(−6)			6.47(−6)	−1.43(−6)	7.50(−6)
0.18725	−5.089(−4)	3.93(−6)			6.44(−6)	−1.43(−6)	7.48(−6)
0.18745	−1.089(−4)	3.94(−6)			6.42(−6)	−1.42(−6)	7.46(−6)
0.18750	−8.891(−6)	3.93(−6)			6.41(−6)	−1.43(−6)	7.47(−6)
0.18775	4.911(−4)	3.93(−6)			6.38(−6)	−1.43(−6)	7.45(−6)
0.18800	9.911(−4)	3.94(−6)			6.36(−6)	−1.43(−6)	7.42(−6)
			$E = 0.005$ a.u.				
0.1850	−5.227(−3)	9.94(−5)	2.3(−7)		1.67(−4)	−3.55(−5)	1.91(−4)
0.1865	−2.224(−3)	9.84(−5)	2.2(−7)		1.63(−4)	−3.56(−5)	1.89(−4)

TABLE II. (*Continued.*)

ω	Δ	Ω	β	γ_1	γ_2	δ_1	δ_2
			$E=0.005$ a.u.				
0.1870	$-1.223(-3)$	$9.81(-5)$	$2.3(-7)$		$1.62(-4)$	$-3.57(-5)$	$1.88(-4)$
0.1875	$-2.225(-4)$	$9.78(-5)$	$2.2(-7)$		$1.60(-4)$	$-3.58(-5)$	$1.87(-4)$
0.1880	$7.785(-4)$	$9.80(-5)$	$2.6(-7)$		$1.59(-4)$	$-3.58(-5)$	$1.86(-4)$
0.1885	$1.779(-3)$	$9.83(-5)$	$2.5(-7)$		$1.58(-4)$	$-3.59(-5)$	$1.85(-4)$
0.1900	$4.782(-3)$	$9.93(-5)$	$2.4(-7)$		$1.54(-4)$	$-3.60(-5)$	$1.82(-4)$
0.1950	$1.479(-2)$	$1.03(-4)$	$2.1(-7)$		$1.41(-4)$	$-3.66(-5)$	$1.73(-4)$
			$E=0.010$ a.u.				
0.1850	$-5.909(-3)$	$3.93(-4)$	$3.9(-6)$		$6.72(-4)$	$-1.42(-4)$	$7.67(-4)$
0.1865	$-2.898(-3)$	$3.89(-4)$	$3.4(-6)$		$6.54(-4)$	$-1.43(-4)$	$7.55(-4)$
0.1870	$-1.895(-3)$	$3.88(-4)$	$3.4(-6)$		$6.49(-4)$	$-1.43(-4)$	$7.52(-4)$
0.1875	$-8.925(-3)$	$3.87(-4)$	$3.4(-6)$		$6.43(-4)$	$-1.44(-4)$	$7.49(-4)$
0.1880	$1.129(-4)$	$3.86(-4)$	$3.9(-6)$		$6.33(-4)$	$-1.43(-4)$	$7.44(-4)$
0.1885	$1.117(-3)$	$3.87(-4)$	$4.0(-6)$		$6.31(-4)$	$-1.43(-4)$	$7.44(-4)$
0.1900	$4.126(-3)$	$3.91(-4)$	$3.9(-6)$		$6.16(-4)$	$-1.44(-4)$	$7.29(-4)$
0.1950	$1.416(-2)$	$4.05(-4)$	$3.3(-6)$		$5.66(-4)$	$-1.47(-4)$	$6.95(-4)$
			(c)				
			$E=0.0010$ a.u.				
0.14810	$-1.582(-4)$	$2.71(-8)$			$3.31(-6)$	$-1.30(-6)$	$1.24(-5)$
0.14812	$-9.816(-5)$	$2.67(-8)$			$3.31(-6)$	$-1.30(-6)$	$1.24(-5)$
0.14184	$-3.816(-5)$	$2.69(-8)$			$3.31(-6)$	$-1.30(-6)$	$1.24(-5)$
0.14816	$2.184(-5)$	$2.68(-8)$			$3.30(-6)$	$-1.30(-6)$	$1.24(-5)$
0.14817	$5.184(-5)$	$2.69(-8)$			$3.30(-6)$	$-1.30(-6)$	$1.24(-5)$
0.14820	$1.418(-4)$	$2.69(-8)$			$3.30(-6)$	$-1.30(-6)$	$1.24(-5)$
			$E=0.0050$ a.u.				
0.14790	$-1.083(-3)$	$3.27(-6)$	$1.6(-8)$		$8.27(-5)$	$-3.24(-5)$	$3.07(-4)$
0.14822	$-1.222(-4)$	$3.24(-6)$	$1.7(-8)$		$8.20(-5)$	$-3.24(-5)$	$3.05(-4)$
0.14825	$-3.208(-5)$	$3.24(-6)$	$1.7(-8)$		$8.19(-5)$	$-3.24(-5)$	$3.05(-4)$
0.14828	$5.804(-5)$	$3.23(-6)$	$1.6(-8)$		$8.19(-5)$	$-3.24(-5)$	$3.05(-4)$
0.14830	$1.181(-4)$	$3.23(-6)$	$1.6(-8)$		$8.19(-5)$	$-3.24(-5)$	$3.05(-4)$
0.14860	$1.019(-3)$	$3.20(-6)$	$1.7(-8)$		$8.12(-5)$	$-3.25(-5)$	$3.04(-4)$
			$E=0.010$ a.u.				
0.1482	$-1.092(-3)$	$2.32(-5)$	$4.9(-7)$		$3.20(-4)$	$-1.30(-4)$	$1.12(-3)$
0.1484	$-4.903(-4)$	$2.31(-5)$	$4.9(-7)$		$3.19(-4)$	$-1.30(-4)$	$1.12(-3)$
0.1485	$-1.893(-4)$	$2.30(-5)$	$4.9(-7)$		$3.18(-4)$	$-1.30(-4)$	$1.11(-3)$
0.1487	$4.134(-4)$	$2.29(-5)$	$4.8(-7)$		$3.16(-4)$	$-1.30(-4)$	$1.11(-3)$
0.1488	$7.144(-4)$	$2.28(-5)$	$4.8(-7)$		$3.16(-4)$	$-1.30(-4)$	$1.11(-3)$
0.1491	$1.618(-3)$	$2.26(-5)$	$4.7(-7)$		$3.13(-4)$	$-1.30(-4)$	$1.11(-3)$

[a]The number enclosed in parentheses indicates the exponent of the multiplicative factor of 10.

values for β we obtain in the three- and four-photon cases when $E=0.001$ a.u. are unreliable. The fits of the Floquet data by the two-level models establish the vaidity of these models for the three physical situations at hand. At the same time the parameters of Table II summarize a great deal of physics, as will become clear in Secs. IV—VII.

The neglect of various terms in the expression for $C(t)$ in Secs. III A and III B is justified numerically by calculating several representative terms and find-
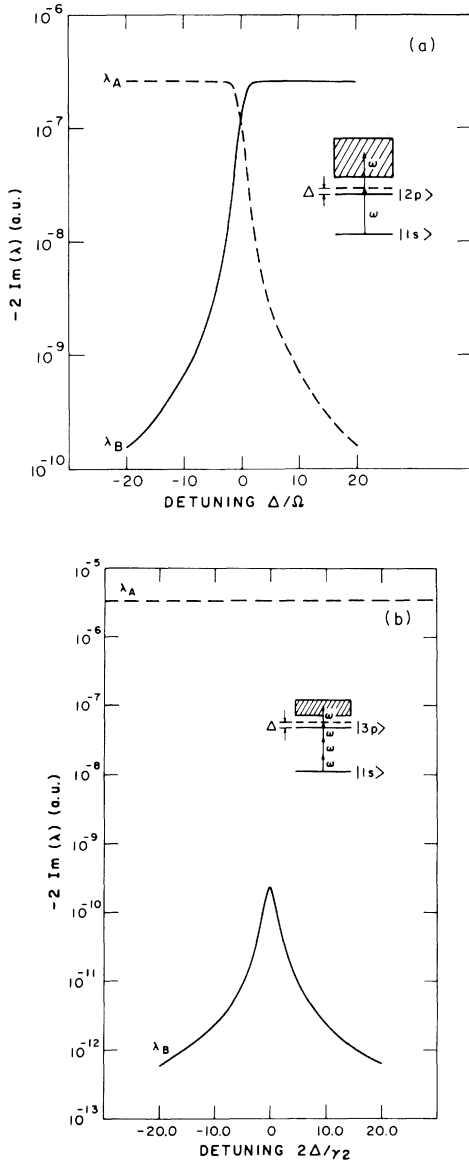
FIG. 2. Imaginary parts of the eigenvalues plotted as a function of detuning for the (a) two- and (b) four-photon ionization of $1s$ state in atomic hydrogen. Two-level parameters used in the plots were obtained from Table II for $E=0.001$ a.u. Note that the imaginary parts cross in (a) but avoid crossing in (b).

ing them to be small. Without reproducing the calculations, we simply state that the truncated terms are found to be less than or equal to E^2, which for $E \ll 1$ a.u. is very small. This observation along with the results in Table II allows one to conclude that the two-level approximation for two-photon ionization of the $1s$ state is very good even at high fields ($E \sim 0.01$ a.u. $\sim 7.0 \times 10^{12}$ W/cm^2).

IV. AVOIDED CROSSINGS OF FLOQUET EIGENVALUES

The complex Floquet eigenvalues dictate the time dependence; accordingly, a qualitative understanding of the frequency dependence of the eigenvalues is needed before an analysis of the time evolution can be made.

Figures 2(a) and 2(b) show the imaginary part of λ_A and λ_B as a function of laser detuning Δ $[=(N-1)\omega-(E_2^{(0)}+\delta_2-E_1^{(0)}-\delta_1)]$, for the two processes ($\Omega \ll \gamma_2$, $\Omega \gg \gamma_2$). In both cases there is an avoided crossing of the eigenvalues; the real parts avoid each other in the two- and three-photon (not shown) case; the imaginary parts avoid each other in the four-photon case. The fact that for growing ratios of γ_2 and Ω the avoided crossing may shift from the real to the imaginary part of the complex dressed eigenvalue is implicit in the discussion of Ref. 6.

This behavior can be understood by considering approximate expressions for λ_A, λ_B in the limit that $E \lesssim 0.001$ a.u. so that $\beta, \gamma_1 \ll \Omega, \gamma_2$ can be neglected. Define real parameters E_A, E_B, γ_A, and γ_B by

$$\lambda_A = E_A - i\frac{\gamma_A}{2} , \tag{22a}$$

$$\lambda_B = E_B - i\frac{\gamma_B}{2} , \tag{22b}$$

$$\omega_{AB} = E_A - E_B . \tag{22c}$$

Then it can be shown that for $\Omega \gg \gamma_2$ (two-photon case),

$$\omega_{AB} \cong (\Delta^2 + \Omega^2)^{1/2} , \tag{23a}$$

$$\gamma_A \cong \frac{\gamma_2}{2} - \frac{\Delta\gamma_2}{2(\Delta^2+\Omega^2)^{1/2}} , \tag{23b}$$

$$\gamma_B \cong \frac{\gamma_2}{2} + \frac{\Delta\gamma_2}{2(\Delta^2+\Omega^2)^{1/2}} . \tag{23c}$$

From Eq. (23a) we see that on resonance ($\Delta=0$) the real parts of λ_A and λ_B differ by the Rabi frequency Ω, and the imaginary parts are equal, $\gamma_A = \gamma_B = \gamma_2/2$ [compare with Fig. 2(a)]. In the opposite limit, $\Omega \ll \gamma_2$ (four-photon case), we have

$$\omega_{AB} \cong -\Delta , \tag{24a}$$

$$\gamma_A \cong \gamma_2 - \frac{\Omega^2\gamma_2}{4[\Delta^2+(\gamma_2^2/4)]} , \tag{24b}$$

$$\gamma_B \cong \frac{\Omega^2\gamma_2}{4[\Delta^2+(\gamma_2^2/4)]} . \tag{24c}$$

Here, on resonance, the real parts of λ_A and λ_B are equal [Eq. (24a)], where the imaginary parts differ;

more precisely we have $\gamma_A \gg \gamma_B$ [compare with Fig. 2(b)]. In the intermediate situation (e.g., the three-photon case) $\Omega \sim \gamma_2$, no such approximations are possible for all detunings. Nevertheless, it can be shown that on resonance $\lambda_A - \lambda_B = [\Omega^2 - (\gamma_2^2/4)]^{1/2}$.

For future reference, note that the following approximation are valid for large $|\Delta|$ $(-\Delta \gg \Omega, \gamma_2)$ regardless of the relative values of Ω and γ_2:

$$\gamma_A \cong \gamma_2 , \tag{25a}$$

$$\gamma_B \cong \frac{\Omega^2 \gamma_2}{4\Delta^2} , \tag{25b}$$

$$\omega_{AB} \cong -\Delta . \tag{25c}$$

Equations (25) show that in the limit of large detunings the dressed-state eigenvalues approach the uncoupled values of the complex atomic energies, as expected.

In Sec. V it will be shown how the behavior of the eigenvalues as a function of detunings and Ω, γ_2 determines the time evolution of the system.

V. TIME DEPENDENCE OF THE IONIZATION RATE

In this section we determine the time scales, detunings, and values of Ω, γ_2 for which a time-independent ionization rate R (as opposed to a long-time ionization rate constant k) can be defined. Ionization rates, rate constants, and time dependences, within the two-level model, have been studied previously[7-9]; nevertheless, we employ a new method to obtain similar rate expressions and time dependence.

Consider first the time-dependent ionization rate $dC(t)/dt$, to determine under what conditions it becomes approximately time independent: From Eq. (8)

$$\frac{dC(t)}{dt} = -\dot{a}_1 a_1^* - a_1 \dot{a}_1^* - \dot{a}_2 a_2^* - a_2 \dot{a}_2^* . \tag{26}$$

Substitution of $\dot{a}_1$ and $\dot{a}_2$ from Eq. (3) gives

$$\frac{dC(t)}{dt} = \gamma_1 |a_1(t)|^2 + \gamma_2 |a_2(t)|^2$$

$$+ \beta(a_1 a_2^* + a_1^* a_2) . \tag{27}$$

For fields $E \lesssim 0.001$ a.u. we can neglect γ_1 and β in Eq. (27) provided that $|2\rangle$ is sufficiently populated; thus

$$\frac{dC(t)}{dt} \cong \gamma_2 |a_2(t)|^2 . \tag{28}$$

This expression has a simple interpretation: $dC(t)/dt$ is the product of the ionization rate out of $|2\rangle$ and the population in $|2\rangle$. Substituting $a_2(t)$

from Eq. (6b), we see that Eq. (28) becomes

$$\frac{dC(t)}{dt} = \gamma_2 \frac{|h_{12}|^2}{|\lambda_A - \lambda_B|^2}$$

$$\times [e^{-\gamma_A t} + e^{-\gamma_B t}$$

$$-2e^{-(\gamma_A + \gamma_B)t/2} \cos(\omega_B t)] . \tag{29}$$

The time behavior of $dC(t)/dt$ on resonance [as given by Eq. (29)] is qualitatively different for the three processes under study. When $\Omega \gg \gamma_2$ (two-photon case), $dC(t)/dt$ is a rapidly oscillating function of time, enveloped by a slower exponential decay [see Eqs. (23)]. When $\Omega \gg \gamma_2$ (four-photon case), $dC(t)/dt$ decays exponentially [see Eq. (24)]. When $\Omega \gtrsim \gamma_2/2$ (three-photon case), oscillation and decay take place on similar time scales. The three cases then correspond to the classical problem of an underdamped, overdamped, and critically damped oscillator.[10]

Despite the oscillatory behavior of the ionization rate in some cases, an approximate time-independent ionization rate exists and hence a cross section can be defined. Figures 3(a)–3(c) display the logarithm of the ionization probability $C(t)$ [from Eqs. (6a), (6b), and (8)] versus log(t) for various laser detunings. Far off resonance $|\Delta| \gg \Omega, \gamma_2$, we see that $C(t)$ is approximately linear (indicated in a double-logarithmic plot by slope 1) in time over a restricted time interval. This interval is shortened as resonance is approached and vanishes altogether in the three-photon case. The time-independent ionization rate R is given by the slope of $C(t)$ in the linear region.

Simple expressions for this rate and time interval can be obtained by suitably approximating the exact rate [Eq. (27) or (29)] and then integrating it over the appropriate time interval to obtain an average rate.

Consider the case of $\Omega \ll \gamma_2$ (four photon). With $\gamma_A \gg \gamma_B$ [Eqs. (24b) and (24c)], for all detunings, the time interval can be restricted so that $\gamma_A t \sim \gamma_2 t \gg 1$ and $\gamma_B t \ll 1$. Hence $dC(t)/dt$, from Eq. (29), is approximately given by

$$\frac{dC(t)}{dt} \cong \frac{\gamma_2 |h_{12}|^2}{|\lambda_A - \lambda_B|^2} . \tag{30}$$

Here the time-independent ionization rate R is given simply by

$$R = \frac{\gamma_2 \Omega^2}{4[\Delta^2 + (\gamma_2^2/4)]} ,$$

$$\frac{1}{\gamma_2} \ll t \ll \frac{4[\Delta^2 + (\gamma_2^2/4)]}{\Omega^2 \gamma_2} , \tag{31}$$
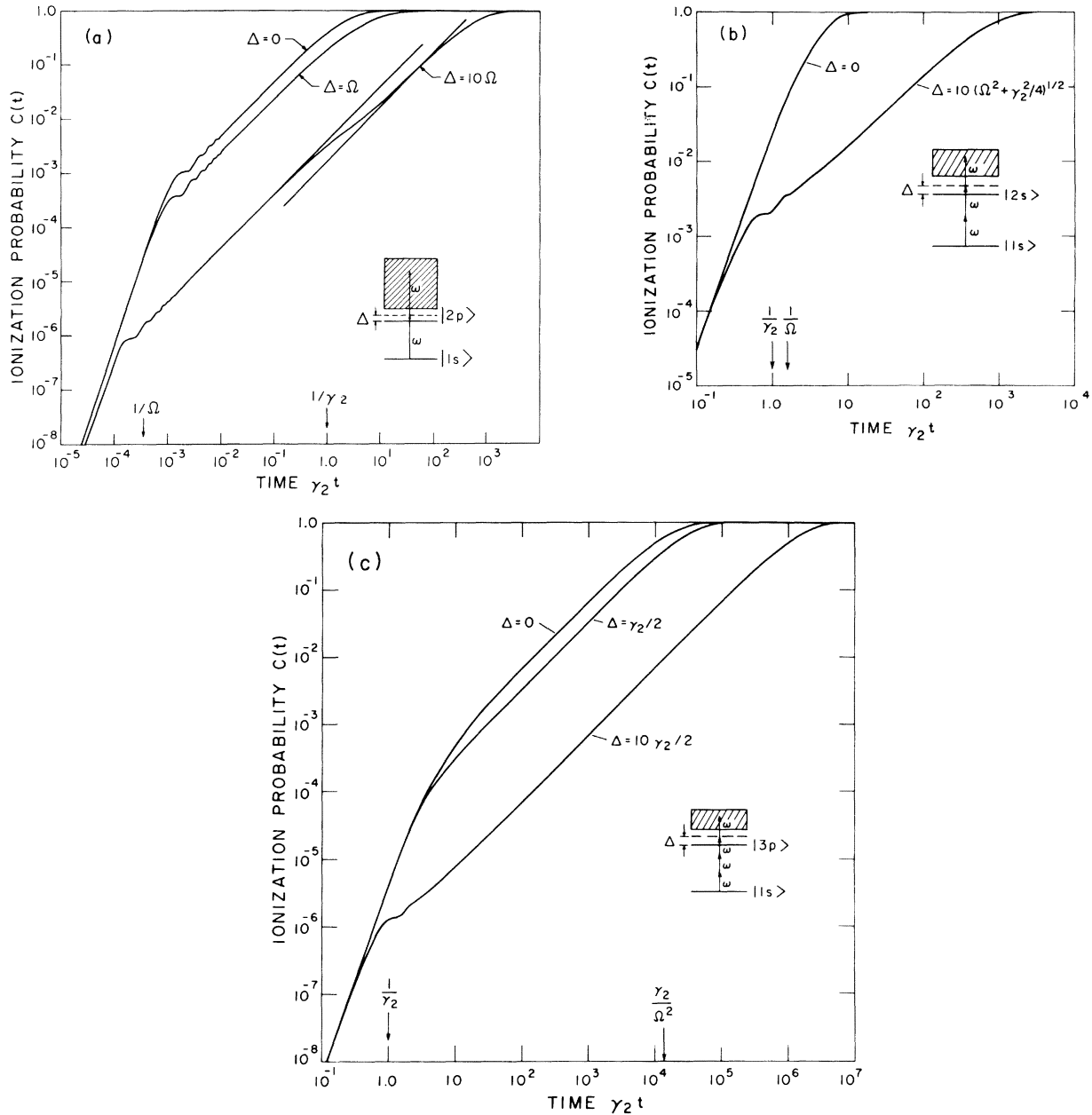
FIG. 3. Ionization probabilities as a function of time for various laser detunings Δ, in the cases of two-, three-, and four-photon ionization of hydrogen discussed in the text. For short times, $C(t)$ is cubic in t (indicated by slope 3) in all three cases. This region is followed by transients which soon become negligible. Linear region (slope 1) ensues in the two- (a) and four-photon (c) cases for all Δ, but only for large Δ in the three-photon case (b). Two linear regions are apparent in the two-photon case, the second appearing when $\gamma_2 t \gg 1$. At large times population depletion occurs which accounts for the exponential approach to one in all three cases. Values of β, Ω, γ_2, and γ_1 were obtained from Table II for (a) $\omega = 0.375$, (b) $\omega = 0.1875$, and (c) $\omega = 0.148\,14$ with $E = 0.001$ a.u. γ_1 was chosen to be zero for three- and four-photon cases and scaled down as E^4 for the two-photon case from the $E = 0.01$ a.u. value. Similarly, β was scaled down as E^{N+1} for the three- and four-photon case from its value at $E = 0.01$ a.u.

where Eq. (24) has been used to approximate $\lambda_A - \lambda_B$, and β is neglected in $|h_{12}|^2$. For restricted times $C(t) \cong Rt$ gives very good agreement with the exact plots of $C(t)$ displayed in Fig. 3(c).

When $\Omega \gg \gamma_2$ (two photon) the rate expression and the time interval are different from Eq. (31). The same time interval cannot be used because γ_A and γ_B become comparable close to resonance. In-

stead, we demand that $\gamma_2 t \ll 1$; then Eq. (29) becomes

$$\frac{dC(t)}{dt} \cong \frac{2\gamma_2 |h_{12}|^2}{|\lambda_A - \lambda_B|^2}[1 - \cos(\omega_{AB}t)] . \qquad (32)$$

The oscillatory term will contribute negligibly to $C(t)$ after times sufficiently long, $\omega_{AB}t \gg 1$. The time-independent ionization rate R is thus given by

$$R = \frac{\Omega^2 \gamma_2}{2(\Delta^2 + \Omega^2)}, \quad \frac{1}{(\Delta^2 + \Omega^2)^{1/2}} \ll t \ll \frac{1}{\gamma_2} \qquad (33)$$

where Eqs. (23) have been used to approximate $\lambda_A - \lambda_B$, and β is neglected in $|h_{12}|^2$. Figure 3(a) indicates the oscillations in $C(t)$ become negligible upon entering the above time interval. In addition, note that in the far-off-resonance curve, a later time interval exists during which a different ionization rate is needed. At large detunings Eqs. (23b) and (23c) show that $\gamma_2 \approx \gamma_A \gg \gamma_B$ ($\Delta < 0$); this allows the restriction of the time interval as in the four-photon case: $\gamma_A t \approx \gamma_2 t \gg 1$ and $\gamma_B t \cong (\Omega^2 \gamma_2/4\Delta^2)t \ll 1$. The ionization rate R, for large detunings, is thus given by

$$R = \frac{\Omega^2 \gamma_2}{4(\Delta^2 + \Omega^2)}, \quad \frac{1}{\gamma_2} \ll t \ll \frac{4\Delta^2}{\Omega^2 \gamma_2} . \qquad (34)$$

This rate is half that in Eq. (33) because for times larger than $1/\gamma_2$ one of the dressed states has become depleted, thus cutting the number of ionization channels in half. Furthermore, had we assumed an adiabatic turn-on with respect to $|2\rangle$, only one linear region would occur, and the rate would be given by Eq. (34).[7]

$C(t) \cong Rt$, with R given by Eqs. (33) and (34), gives a good approximation to the $C(t)$ appearing in Fig. 3(a). Nevertheless, more accurate rates are obtained by including the contributions of β and γ_1 in Eq. (27) and then preceding as before. We simply present the results,

$$R = \frac{\gamma_2 \Omega^2}{2(\Delta^2 + \Omega^2)} \left[1 - \frac{2\beta\Delta}{\Omega\gamma_2} + \frac{2\Delta^2 \gamma_1}{\gamma_2 \Omega^2} \right] ,$$

$$\frac{1}{(\Delta^2 + \Omega^2)^{1/2}} \ll t \ll \frac{1}{\gamma_2} , \qquad (35)$$

and for $|\Delta| \gg \Omega$,

$$R = \frac{\gamma_2 \Omega^2}{4(\Delta^2 + \Omega^2)} \left[1 - \frac{4\beta\Delta}{\Omega\gamma_2} + \frac{4\Delta^2 \gamma_1}{\gamma_2 \Omega^2} \right] ,$$

$$\frac{1}{\gamma_2} \ll t \ll \frac{4\Delta^2}{\Omega^2 \gamma_2} . \qquad (36)$$

$C(t) \cong Rt$, with R now given by Eqs. (35) and (36), gives a very good approximation to the $C(t)$ appearing in Fig. 3(a). It is clear, from Eqs. (35) and (36), that there is an asymmetry in the line shapes caused by the parameter β. This asymmetry in the profile appears in three- and four-photon cases, but only at very large detunings. In this case the rate in Eq. (31) is supplemented to give ($\Omega \ll \gamma_2$)

$$R = \frac{\gamma_2 \Omega^2}{4\Delta^2} \left[1 - \frac{4\beta\Delta}{\Omega\gamma_2} + \frac{4\gamma_1 \Delta^2}{\gamma_2 \Omega^2} \right] ,$$

$$\frac{1}{\gamma_2} \ll t \ll \frac{4\Delta^2}{\Omega^2 \gamma_2} . \qquad (37)$$

For the remaining case $\Omega \gtrsim \gamma_2/2$, no time-independent ionization rate exists for all detunings. Only in the far-off-resonance case $|\Delta| \gg \Omega, \gamma_2$, where $\gamma_A \gg \gamma_B$ ($\Delta < 0$), can one demand that $\gamma_2 t \approx \gamma_A t \gg 1$ and $\gamma_B t \cong (4\Delta^2/\Omega^2 \gamma_2)t \ll 1$. The resulting rate is identical to Eq. (37) and gives very good agreement when compared with the $\Delta = 10[\Omega^2 + (\gamma_2^2/4)]^{1/2}$ plot in Fig. 3(b).

The time behavior of $C(t)$ outside the above time intervals, as displayed in Figs. 3, can be understood with the help of Eqs. (6b), (28), and (29). For early times $(t \ll 1/\omega_{AB}, 1/\gamma_2)$, $|a_2(t)| \cong |h_{12}|t$, [Eq. (6b)], and the approximate rate $dC(t)/dt$ is given by Eq. (28),

$$\frac{dC(t)}{dt} \cong \frac{\Omega^2 \gamma_2 t^2}{4} ; \qquad (38)$$

thus $C(t) \cong \Omega^2 \gamma_2 t^3/12$. This expression is accurate in the time regimes of Fig. 3 where the slope is 3. For much later times, $t \gg 1/\gamma_2, 4\Delta^2/\Omega^2 \gamma_2$, exponential depletion of the bound-state populations has occurred. This regime is marked, in Fig. 3, by the asymptotic approach of $C(t)$ to 1. The long-time ionization rate constant k governing this depletion region is given approximately by $\gamma_m \equiv \min\{\gamma_A, \gamma_B\}$. γ_m is not in general equal to any of the above calculated R's. Only in the four-photon case is $\gamma_m \cong R$ [Eqs. (31) and (37)]. In the two-photon case we find that on resonance $\gamma_m \cong R$ [Eq. (35)], far off resonance $\gamma_m \cong R$ [Eq. (36)], but neither R is valid in the intermediate case. On the other hand, the on-resonant oscillations in $C(t)$ for the three-photon case make the approximation $C(t) \cong 1 - e^{-\gamma_m t}$ only fair (see Fig. 4). Furthermore, $\gamma_m \cong R$ [Eq. (37)] only far off resonance.

There are three qualitatively different time regimes[9] exhibited in Figs. 3. At early times $C(t)$ is cubic in t, follwed by linear regime (except in the three-photon case), and finally the depletion region where $C(t) \cong 1 - e^{-\gamma_m t}$. Only in the linear regime is
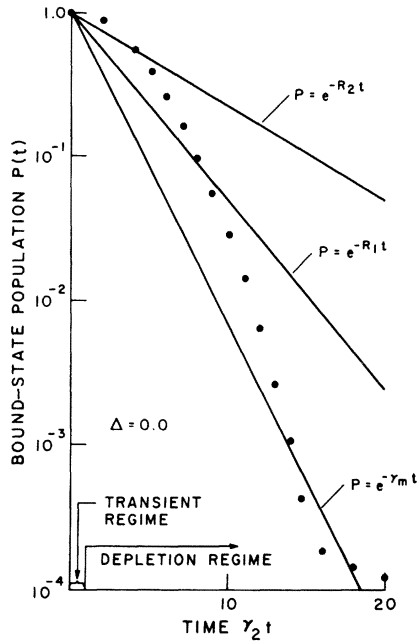
FIG. 4. Time dependence of bound-state populations P, for three-photon ionization of the $1s$ state at large times $(\gamma_2 t \gg 1)$ for $\Delta = 0.0$. Points lie on the curve given by $P_e = |a_1|^2 + |a_2|^2$ as defined in Eq. (6); $R_1 = \gamma_2 \Omega^2 / 2(\Delta^2 + \Omega^2)$ and $R_2 = \frac{1}{2}R_1$, γ_m is as defined in the text. Nonexponential behavior of P_e at $\Delta = 0$ occurs because the oscillations are comparable to the exponential depletion. These calculations utilize the parameters from Table II(b) for $E = 0.001$ and $\omega = 0.1875$.

a cross section defined. In Figs. 5 and 6 we compare our cross sections with those of other authors.

Generalized cross sections for the two-photon ionization of atomic hydrogen appear in Fig. 5. Assuming that $1/\Omega \ll t \ll 1/\gamma_2$, we use the rate R from Eq. (35) and the frequency-dependent parameters from Table II in the calculation. These cross sections are in good agreement with those obtained by Chu and Reinhardt[1] except in the frequency domain where interference from the $3p$ level becomes important. In this latter domain, the two-level model is inadequate.

A special case occurs whenever $\Omega \sim \gamma_2$ and $\Delta = 0$. The end of the cubic region marks the beginning of the depletion region; hence no linear region exists, and therefore no time-independent rate (i.e., cross section) exists. Nevertheless, a cross section can be defined which is valid off resonance and plausible (by the arguments above) on resonance. Using γ_m as the ionization rate, cross sections for this process are plotted in Fig. 6. Contrary to perturbation theory, the generalized cross sections are intensity dependent, but are seen to agree with Maquet's[11] results at low fields. Our results differ from Maquet's in the
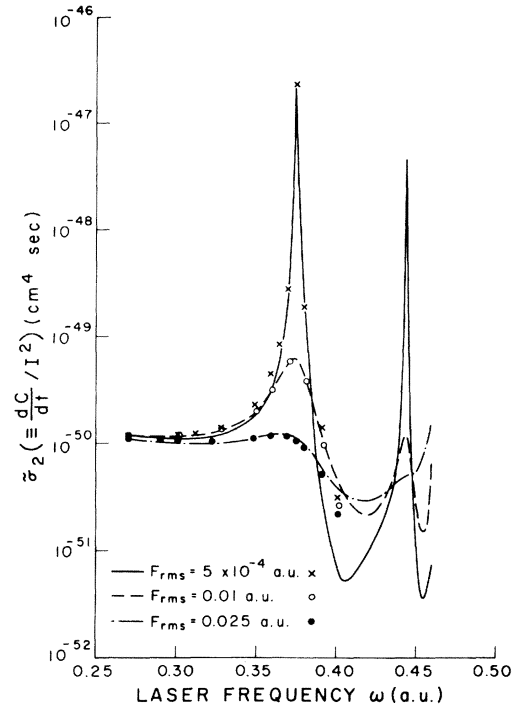
FIG. 5. Cross sections for two-photon ionization of the $1s$ state in hydrogen at three intensities. Points are the cross sections calculated using the rate expression Eq. (35) and the frequency-dependent parameters from Table II. Curves are the generalized Floquet results of Chu and Reinhardt (Ref. 1). They have utilized the ionization rate dC/dt, where $C(t)$ is obtained from Eq. (9) (sum over β includes only the $1s$, $2p$, and $3p$ states). Rapidly oscillating terms have been neglected for reasons discussed in the text. We see that the two-level model is valid except in a frequency domain $(\omega \geq 0.390$ a.u.) where interference effects from the $3p$ level become important.

frequency domain where interference effects from the $3s$ level become important: Here the two-level approximation is expected to be invalid.

Alternate methods of comparing theory and experiment have evolved in the form of the "K index." In Sec. VI, the K index is discussed in the context of the two-level model with application to atomic hydrogen.

VI. K INDEX

Experimental results, and recently theoretical studies,[3] of multiphoton ionization have been presented in the form of K-index plots, in which

$$K = \frac{\partial \ln N_i}{\partial \ln I} \tag{39}$$

is plotted as a function of Δ. N_i is the number of ions per laser pulse, and I is the laser intensity. N_i,
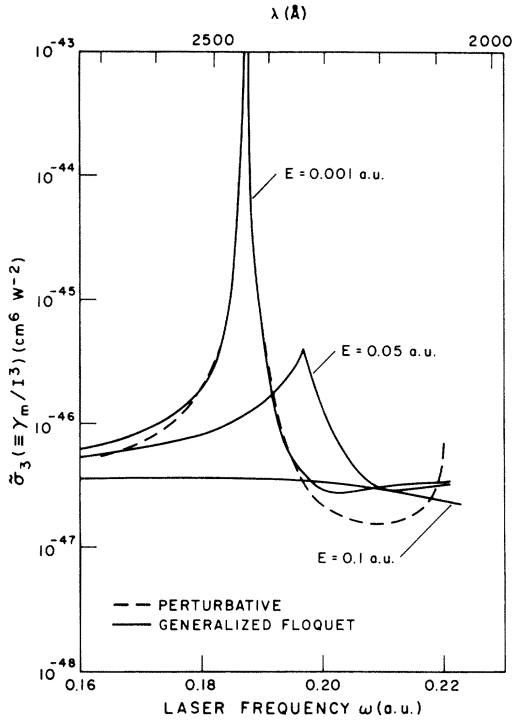
FIG. 6. Cross sections for three-photon ionization of the $1s$ state at three laser intensities. γ_m is used as the ionization rate and calculated within the two-level model using parameters from Table II(b). For β and γ_1 we chose their far-off-resonant $(\omega = 0.1850$ a.u.$)$ values at $E = 0.01$ a.u. and scaled by the appropriate power of E. These values were chosen because β and γ_1 only become important far off resonance. At low fields, $E \leq 0.001$ a.u. $\sim 3.5 \times 10^{10}$ W/cm^2 (rms), and large detunings $(\omega < 1850$ a.u.$)$ our results agree with the perturbative results of Maquet (Ref. 11). Disagreement occurs as interference effects of the $3s$ level become important $(\omega \geq 0.1950$ a.u.$)$. At high fields, $E \geq 0.05$ a.u. $\sim 8.8 \times 10^{13}$ W/cm^2 (rms), the power dependence of the cross sections is evident and disagrees with perturbation theory.

and therefore K, will depend not only on the detuning but also on the pulse duration t and the relative values of the atomic parameters.

Figure 7 shows K-index plots, at fixed values of t, for the three different ionization processes under study. The plots were made assuming that $N_i = N_i(0) C(t)$, where $N_i(0)$ is the number of atoms at $t = 0$ and $C(t)$ is as defined earlier. Figures 7(a) and 7(c) also show curves labeled "rate curve." They are obtained assuming $C(t) \cong Rt$, where R is proportional to $dC(t)/dt$ in Eq. (30). The proportionality constant is either 1 or 2 depending on the process. A simple analytic expression[12] is thus obtained for the rate curve $K_{(rate)}$,

$$K_{(rate)} = N + \frac{2\Delta(\delta_2 - \delta_1) - \gamma_2^2/2 - (N-1)\Omega^2}{\Delta^2 + (\gamma_2^2/4) + \Omega^2} ,$$

$$(40)$$

where β and γ_1 have been neglected and $|\lambda_A - \lambda_B|^2 \cong \Delta^2 + \Omega^2 + \gamma_2^2/4$, valid for both $\Omega \gg \gamma_2$ and $\Omega \ll \gamma_2$. Note that $K_{(rate)}$ is the sum of a Lorentzian and a dispersionlike curve and that for large detuning $(|\Delta| \gg \Omega, \gamma_2)$ $K_{(rate)}$ becomes the number of photons N needed to ionize the atom.

$K_{(rate)}$ is to be compared with the exact plots of K displayed in Fig. 7. In the four-photon case $(\Omega \ll \gamma_2)$, $K_{(rate)}$ is seen to exactly agree with K for times t in the linear region [see Eq. (31)]; at short times K flattens out to a constant value of 4; at long times K distorts from $K_{(rate)}$ but still maintains its dispersionlike quality.

The negative values of K indicate that for a fixed laser frequency ω the number of ions actually decreases as the laser intensity increases. This surprising feature can occur when the ac Stark shift is comparable to the linewidth. If the line center is shifted away from the fixed frequency, then the number of ions may decrease with intensity; on the other hand, a shift towards the fixed frequency results in an increase in the number of ions with intensity. These considerations account for the negative and large positive values of K on either side of resonance.

In the two-photon case $(\Omega \gg \gamma_2)$ new features appear [Fig. 7(a)]. The dispersionlike quality is not present because the relatively large half-width $(\Omega \gg \delta_1, \delta_2)$ makes such effects negligible. The rapid oscillations in the exact K-index plot [Fig. 7(a)] are understood with the help of Eqs. (23a) and (32). Assuming that, in the linear region, $C(t)$ is approximately given by the integral over time of Eq. (32), K becomes, after suitable approximations,

$$K \cong K_{(rate)} - \frac{1}{2} \frac{\Omega^2 \cos[(\Delta^2 + \Omega^2)^{1/2} t]}{\Delta^2 + \Omega^2} .$$

$$(41)$$

Equation (41) shows that K oscillates in the frequency domain about $K_{(rate)}$ with a period that decreases with time. Those oscillations of K are measurable only if the oscillations of $C(t)$ in Fig. 3(a) are measurable, otherwise $K \cong K_{(rate)}$.

Both dispersion and oscillatory features are present in the K-index plots for the intermediate three-photon case $(\Omega \geq \gamma_2/2)$ [Fig. 7(b)], but only for times $t \sim 1/\Omega$, $1/\gamma_2$. Dispersion dominates at slightly longer times and $K \cong 3$ at slightly shorter times.

Both the time behavior and the K-index profile are determined principally by the relative values of Ω and γ_2. When K is dispersionlike
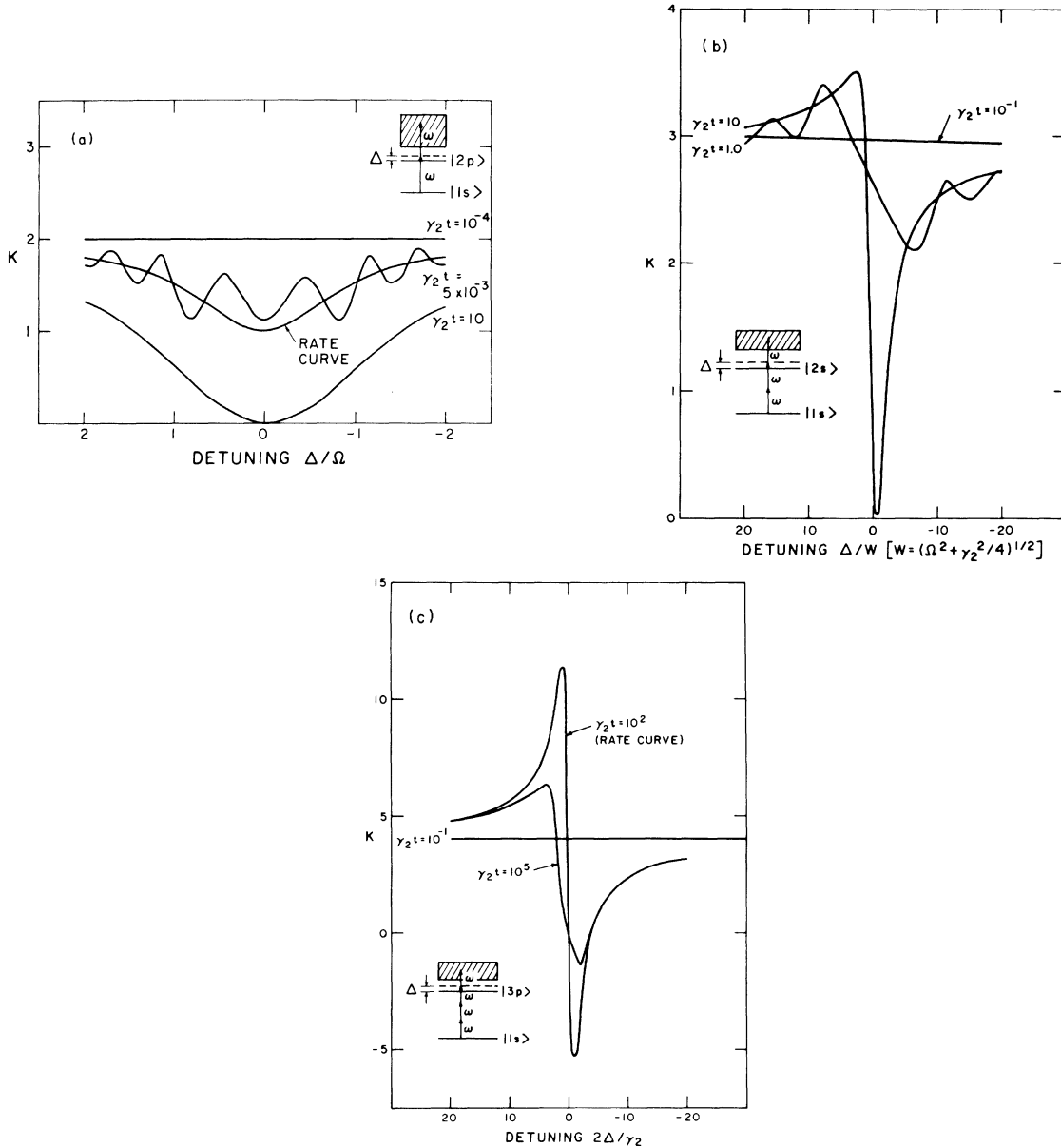
FIG. 7. K as a function of laser detuning for (a) two-, (b) three-, and (c) four-photon ionization, where $K = \partial \ln C(t)/\partial \ln I$ [$C(t)$ is the ionization probability] for several values of t (laser pulse length). Rate curves are obtained assuming $C(t) = Rt$, where R is the approximate ionization rate obtained in the text. For large Δ, K approaches the number of photons necessary for ionization. Oscillations in (a) are attributable to the relatively large value of Ω. These oscillations are squeezed together as t increases. K is a dispersionlike curve in (c), a consequence of a relatively large ac Stark shift. Combination of (a) and (c) appears in (b) due to $\Omega \sim \gamma_2 \sim \delta_2, \delta_1$. Appearance of the oscillation depends on the pulse length t.

$(\Omega \ll \gamma_2 \sim \delta_1, \delta_2)$, $dC(t)/dt$ is governed by exponential decay, and when K oscillates $(\delta_1, \delta_2 \sim \gamma_2 \ll \Omega)$, $dC(t)/dt$ oscillates.

VII. MULTILEVEL RESONANCE EFFECTS

The two-level model is inappropriate whenever the population in off-resonant levels becomes comparable to that in $|2\rangle$ or $|1\rangle$. The criterion is made specific by considering an approximate expression for the off-resonant population. With laser turn-on time τ, the maximum population in an off-resonant level $|\beta\rangle$ is given approximately by $[\Omega_{1\beta}/(\Delta_{1\beta}^2\tau)]^2$ in the adiabatic turn-on[13] and by $(\Omega_{1\beta}/\Delta_{1\beta})^2$ in the sudden turn-on [see Eq. (6b)], where $\Omega_{1\beta}$ is the effec-
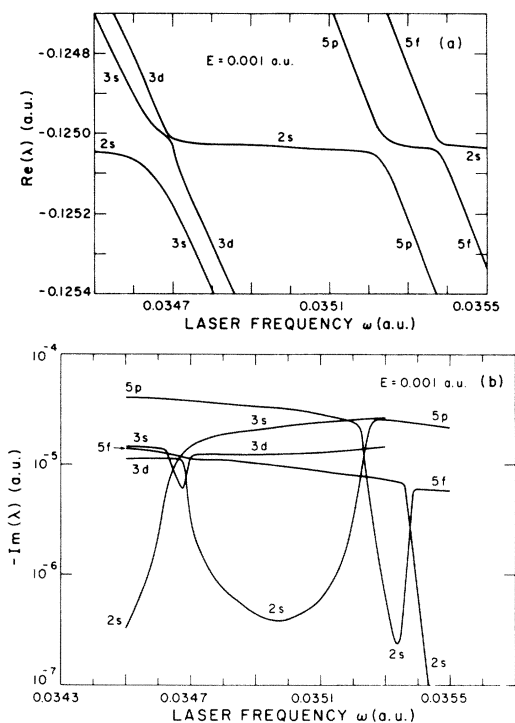
FIG. 8. (a) Real and (b) imaginary parts of the eigenvalues for the resonant four-photon ionization of the $2s$ state described in the text at $E=0.001$ a.u. All real parts avoid each other while the imaginary parts cross; the crossing of the imaginary parts results in an enhancement of the ionization rate. These graphs indicate a breakdown of the two-level model for $E \geq 0.001$ a.u.

tive Rabi frequency connecting $|1\rangle$ and $|\beta\rangle$ and $\Delta_{1\beta}$ the laser detuning from $|\beta\rangle$. The maximum population in $|1\rangle$ and $|2\rangle$, in the two- and three-photon case near resonance, is on the order of unity [see Eq. (6)]; hence the two-level model is suitable provided $|\Omega_{1\beta}/\Delta_{1\beta}|^2 \ll 1$, which is satisifed when $|\beta\rangle$ is far off resonance, *independent* of laser turn-on time.

In the four- or more-photon case, the laser turn-on time becomes critical because the maximum population in $|2\rangle$ is approximately $\Omega^2/\gamma_2^2 \sim E^{2(N-3)}$ $(N \geq 4)$ which is small for $E \ll 1.0$ a.u. The two-level model is suitable only if $\tau \gg \gamma_2 \Omega_{1\beta}/\Delta_{1\beta}^2 \Omega$. As an example, take $\Omega_{1\beta} \sim E$ and $\Delta_{1\beta} \sim 10^{15}$ Hz. Then the above criterion becomes $\tau \gg E^{4-N} \times 10^{-14}$ sec, which for $N=4$ is easily satisfied by real lasers.[14]

We have considered a four-photon process in which other off-resonance levels are close enough so as not to be neglected, regardless of turn-on time. The $2s$ state is ionized by four photons from a linearly polarized, monochromatic laser. The $3s, 3d$ and $5p, 5f$ ($m_l = 0$) levels act as the intermediate resonant states.

Since the eigenvalues determine the time evolution
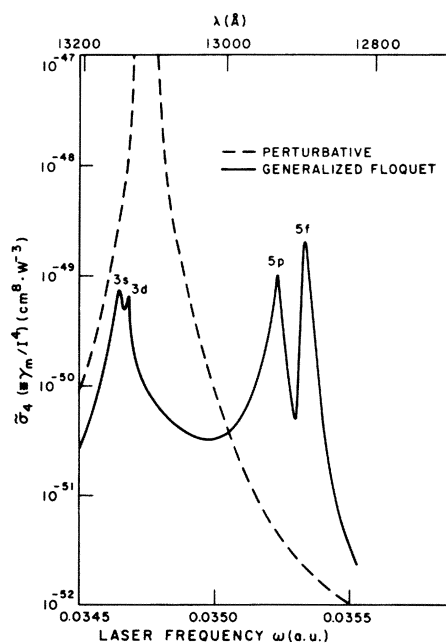
FIG. 9. Cross sections for the four-photon ionzation of the $2s$ state with the $3s, 3d, 5p, 5f$ states in near resonance. Ionization rate γ_m is extracted from Fig. 8(b) by choosing $\gamma_m \equiv 2 \min[-\mathrm{Im}(\lambda_i)]$, where λ_i is the ith eigenvalue in Fig. 8(b). This cross section is compared with the perturbative results of Gontier and Trahin (Ref. 16).

of the process, a study of their behavior as a function of laser frequency is necessary. At low fields $E \leq 0.0001$ a.u. we find the eigenvalues are qualitatively similar to the two-level approximation of a four-photon process in that the real parts cross and the imaginary parts avoid. At higher fields $E=0.001$ a.u. the graphs are quite different (see Fig. 8); the real parts avoid and the imaginary parts cross. This result is qualitatively similar to the three-photon case.

This qualitative change in the time behavior as a function of laser intensity can be viewed as a power broadening of the $n=3$ levels into resonance with the $2s$ and $n=5$ levels. Clearly, the standard two-level model is inadequate to describe this process, and a multilevel generalization of the two-level picture is needed.[15]

Approximate ionization rates can be obtained without analyzing the detailed and complicated time dependence. We saw earlier that the rate constant , given by $\gamma_m \equiv \min\{\gamma_A, \gamma_B\}$, is a reasonable approximation to the time-independent rate R: Thus ionization rates can be extracted from Fig. 8 by defining $\gamma_m \equiv 2 \min[-\mathrm{Im}(\lambda_i)]$ (where λ_i is the ith eigenvalue). The minimization acts only on the λ_i associated with an avoided crossing in Fig. 8. Cross sections are calculated using this rate and displayed in

Fig. 9 (for $E=0.001$ a.u.) along with the perturbative results of Gontier and Trahin.[16]

VIII. CONCLUSION

We have shown that knowledge of the complex eigenvalue of the generalized Floquet Hamiltonian for N-photon resonant ionization of atomic hydrogen ($N=2,3,4$) provides numerical values for the parameters appearing in the two-level model. The numerical values in Table II indicate that the field dependences of these parameters are as predicted by the standard two-level models for $E \leq 0.01$ a.u. $\sim 7.0 \times 10^{12}$ W/cm^2. We also find numerically that (assuming adiabatic square pulse) populations in the other (far-off-resonant) levels are negligible. These results validate the use of the two-level model in these specific cases.

Nevertheless, caution must be exercised: Owing to the small coupling (effective Rabi frequency), other off-resonant levels may significantly influence the dynamics. This has been demonstrated to occur as a function of laser intensity in a particular four-photon ionization process, where the off-resonant levels power broaden so as to overlap the resonant region.

When the two-level approximation is valid, a time-independent ionization rate can be obtained under certain conditions; the laser must be turned on long enough to adequately populate $|2\rangle$ but not long enough to severely deplete the number of atoms. We have shown that, in this interval, the number of ions grows linearly in time for two- and four-photon ionization (and for three-photon ionization far off resonance) of atomic hydrogen. The slope of the ionization probability curve is defined to be the rate, and was seen to be adequately given by Eqs. (31) and (35)–(37). No linear region exists (hence no time-independent rate) in the three-photon case on resonance.

The time-independent ionization rate R is relevant in the linear regime; here the ionization probability $C(t) \cong Rt$. In the depletion regime, on the other hand, $C(t) \cong 1 - e^{-kt}$. We have shown that in general $k \neq R$. We find in the two- and three-photon case $k \cong R$ on and far off resonance but not for intermediate detunings. Nevertheless, $k \cong R$ for all detunings in the four-photon case. This surprising feature is attributable to the complicated short-time behavior of the ionization probability.

The K-index plots have become useful in presenting experimental results. We have shown how the theoretical curves can be understood in terms of relative values of the two-level parameters. The Rabi frequency dominates in the two-photon case, resulting in rapid oscillations of K as a function of the detuning Δ. (This assumes that oscillations in the number of ions can be detected as a function of time. If not, K will simply be an inverted Lorentzian with width Ω.) When the ac Stark shift is comparable to the ionization rate and Ω is negligible, as in the four-photon case, K becomes a dispersionlike curve (K can even be negative). The three-photon ionization is the intermediate case and thus its K-index plot shows both features—oscillations and dispersion. These features appear whenever the two-level approximation is valid.

The main drawback of the present work is the assumption of the rounded square pulse discussed in Ref. 2. Assumption of this particular turning on and off of the assumed monochromatic laser has allowed the analytical work of Secs. III—VI, giving a solid physical and mathematical underpinning to the computed time dependences and K-index dispersion plots. However, provided that one is willing to work numerically, the same analysis can be carried out using the intensity and detuning dependence of parameters of Table II for arbitrary laser pulse and mode structure characteristics.[8,17,18] Only then can detailed comparison with experiment be made.

ACKNOWLEDGMENTS

APPENDIX: COMPLEX SYMMETRIC HAMILTONIAN

Let $|A\rangle$ be a complex-valued column vector and the transposed version of $|A\rangle$ be denoted by $\langle A|$,

$$\langle A| \equiv (|A\rangle)^T . \tag{A1}$$

Note the distinction between these and Dirac brackets: $\langle A|$ is not the adjoint of $\langle A|$ in our notation. Equation (A1) implies that $\langle A|B\rangle = \langle B|A\rangle$.

Consider the following eigenvalue problem:

$$H|A\rangle = \lambda_A |A\rangle , \tag{A2}$$

$$H|B\rangle = \lambda_B |B\rangle , \tag{A3}$$

where H is a symmetric (not necessarily Hermitian) matrix

$$H^T = H .\qquad (A4)$$

The requirement that H be only symmetric allows for complex eigenvalues. To derive the orthogonality relation for symmetry Hamiltonians, we multipy Eq. (A2) by $\langle B |$, Eq. (A3) by $\langle A |$, and subtract, to obtain

$$(\lambda_A - \lambda_B)\langle A | B \rangle = 0 .\qquad (A5)$$

The identity $\langle B | H | A \rangle = \langle A | H | B \rangle$, from Eq. (A4), is used. This equation guarantees that the eigenvectors of a symmetric Hamiltonian are orthogonal.

Care must be taken when calculating $\langle A | B \rangle$ so

as not to confuse it with Dirac brackets. For example, let

$$|A\rangle = \begin{bmatrix} A_1 \\ A_2 \end{bmatrix} ,\qquad (A6)$$

and

$$|B\rangle = \begin{bmatrix} B_1 \\ B_2 \end{bmatrix} ,\qquad (A7)$$

where A_1, A_2 and B_1, B_2 are complex numbers. Then

$$\langle A | A \rangle = A_1^2 + A_2^2 ,\qquad (A8)$$

and

$$\langle B | A \rangle = \langle A | B \rangle = A_1 B_1 + A_2 B_2 .\qquad (A9)$$

*Present address: TRW, 1 Space Park, Building 02, Room 1779, Redondo Beach, California 90278.

†Present address: Institute of Optics, University of Rochester, Rochester, New York 14627.

[1]J. H. Shirley, Phys. Rev. 138, B979 (1965); S.-I Chu and W. P. Reinhardt, Phys. Rev. Lett. 39, 1195 (1977); S.-I Chu, Chem. Phys. Lett. 54, 367 (1978); A. Maquet, S.-I Chu, and W. P. Reinhardt, preceding paper, referred to hereafter as MCR.

[2]An adiabatic square pulse occurs when the field is turned on in a finite time τ to a constant rms intensity. It must be turned on fast compared to the time evolution of the resonant states, but slow compared to that of the far-off-resonance states. This criterion is made specific by demanding $1/|\Delta_{1\beta}| \ll \tau \ll 1/[\Delta^2 + \Omega^2 + (\gamma_2^2/4)]^{1/2}$, where $\Delta_{1\beta}$ is the detuning from the far-off-resonance states and Ω, γ_1, and Δ are as defined in the text. [See E. Courtens and A. Szöke, Phys. Rev. A 15, 1588 (1977).]

[3]J. Morellec, D. Normand, and G. Petite, Phys. Rev. A 14, 300 (1976); Multiphoton Processes, edited by G. Mainfrey, J. H. Eberly, and P. Lambropoulos (Wiley, New York, 1978), p. 253; L. A. Lompre, G. Mainfray, C. Manus, and J. Thebault, Phys. Rev. A 15, 1604 (1977); M. Crance, J. Phys. B 11, 1931 (1978); J. H. Eberly, Phys. Rev. Lett. 16, 1049 (1979).

[4]L. Allen and J. H. Eberly, Optical Resonance and Two-Level Atoms (Wiley, New York, 1975); B. L. Beers and L. A. Armstrong, Phys. Rev. A 12, 2447 (1975); M. Crance and S. Feneuille, ibid. 16, 1587 (1977); P. L. Knight, Opt. Commun. 22, 173 (1977).

[5]Far-off-resonance ionization cross sections and ac Stark shifts have been computed for hydrogen by several authors, e.g., B. A. Zon, N. L. Manakov, and L. P. Rapoport, Opt. Spekstrosk. 38, 13 (1975) [Opt. Spectrosc. 38, 6 (1975)]; W. Zernik, Phys. Rev. A 135, 51 (1964); Y. Gontier and M. Trahin, ibid. 4, 1896 (1971); G. Laplanche, A. Durrieu, Y. Flank, M. Jaouen, and A. Rachman, J. Phys. B 9, 1263 (1976); T. N. Chang and

R. T. Poe, ibid. 9, L311 (1976); B. Ritchie, Phys. Rev. A 17, 659 (1978); S. N. Dixit and P. Lambropoulos, ibid. 19, 1576 (1979).

[6]W. E. Lamb, Jr., Phys. Rev. 85, 259 (1952); V. Gontier and M. Trahin, Phys. Rev. A 19, 264 (1979); C. Cohen-Tannoudji, Cargèse Lectures in Physics (Gordon and Breach, New York, 1967), Vol. 2, pp. 347–393.

[7]B. L. Beers and L. A. Armstrong, Jr., Phys. Rev. A 12, 2447 (1975); A. E. Kazakov, V. P. Makarov, and M. V. Federov, Zh. Eksp. Teor. Fiz. 70, 38 (1976) [Sov. Phys.—JETP 43, 20 (1976)]; J. R. Ackerhalt and B. W. Shore, Phys. Rev. A 16, 277 (1977); J. H. Eberly and S. V. O'Neil, ibid. 19, 1161 (1979).

[8]J. L. F. de Meijere and J. H. Eberly, Phys. Rev. A 17, 1416 (1978).

[9]M. V. Fedorov, J. Phys. B 10, 2573 (1977); M. V. Fedorov and A. E. Kazakov, Opt. Commun. 22, 43 (1977); D. L. Andrews, J. Phys. B 17, L659 (1977); W. A. McClean and S. Swain, ibid. 17, L515 (1978).

[10]J. B. Marion, Classical Dynamics (Academic, New York, 1965), or any elementary classical mechanics book.

[11]A. Maquet, Phys. Rev. A 15, 1088 (1977).

[12]Similar to that obtained by J. H. Eberly, Phys. Rev. Lett. 16, 1049 (1979).

[13]L. I. Schiff, Quantum Mechanics (McGraw-Hill, New York, 1955), p. 291.

[14]We note that this criterion may not be satisfied for larger N and small E ($E \ll 1.0$ a.u.). Take, for example $N = 6$ and $E = 10^{-4}$ a.u. ($\sim 7.0 \times 10^8$ W/cm^2); we must have $\tau \gg 10^{-6}$ sec, a very "long" turn-on time.

[15]See the following for multilevel systems: B. W. Shore and J. R. Ackerhalt, Phys. Rev. A 15, 1640 (1977); W. A. McClean and S. Swain, J. Phys. B 12, 723 (1979).

[16]Y. Gontier and M. Trahin, Phys. Rev. A 7, 2069 (1973).

[17]The laser pulse shape, duration, spontaneous emission, and other effects for real atoms are considered in the following papers: P. Lambropoulos, in Advances in Atomic and Molecular Physics, edited by D. R. Bates

and B. Bederson (Academic, New York, 1976), Vol. 12, pp. 87–164; A. T. Georges and P. Lambropoulos, Phys. Rev. A <u>15</u>, 727 (1977); N. B. Delone and V. P. Krainov, Usp. Fiz. Nauk <u>124</u>, 619 (1978) [Sov. Phys.— Usp. <u>21</u>, 309 (1978)]; P. Agostini, A. T. Georges, S. E. Wheatley, P. Lambropoulos, and M. D. Levenson, J. Phys. B <u>11</u>, 1733 (1978); W. A. McClean and S. Swain, *ibid.* <u>11</u>, 1717 (1978); J. R. Ackerhalt, Phys. Rev. A <u>17</u>, 293 (1978); Y. Gontier and M. Trahin, J. Phys. B <u>11</u>, L131 (1978); C. E. Theodosiou, L. A. Armstrong, Jr., M. Crance, and S. Feneuille, Phys. Rev. A <u>19</u>, 766 (1979); P. Zoller, *ibid.* <u>19</u>, 1151 (1979); Y. Gontier and M. Trahin, J. Phys. B <u>12</u>, 2123 (1979); W. A. McClean and S. Swain, *ibid.* <u>12</u>, 2291 (1979).

[18]This has been carried out for the three-photon problem by K. Scheibner and W. P. Reinhardt (unpublished); K. Scheibner, Ph.D. Thesis, University of Colorado, Boulder, 1983.